

Fractographic evidence of hydrogen transport by diffusion in pearlitic steel

J. TORIBIO*

Department of Materials Science, Polytechnical University of Madrid, ETSI Caminos, Ciudad Universitaria, 28040 Madrid, Spain

Hydrogen embrittlement is a phenomenon of environmentally assisted cracking which appears at a wide range of electrochemical potentials [1]. Clarifying the main mechanism of hydrogen transport in metals is therefore of great importance in hydrogen-assisted cracking. A great research effort has been made in recent years in this area. The problem, however, is not yet fully understood, and two main types of hydrogen transport in metals have been proposed: lattice diffusion [2, 3], according to which hydrogen diffuses not only towards the points of minimum concentration, but also towards those of maximum hydrostatic stress; and dislocation sweeping [4, 5], according to which hydrogen is dragged by dislocations as the plastic zone spreads.

There is, however, a strong controversy about the main mechanism of hydrogen transport in steel and whether dislocation sweeping can be considered an embrittlement mechanism *per se*. In spite of its well-established bases, hydrogen transport by dislocation dragging may not be a critical step for hydrogen embrittlement [6]. Furthermore, Zakroczymski [7] observed no accelerating effect of plastic deformation on hydrogen transport.

This letter tries to establish experimental bases for a mechanism of hydrogen transport by diffusion in pearlitic steels. The research is based on the existence of an unconventional microscopic fracture mode, the tearing topography surface (TTS), so called by Thompson and Chesnutt [8]. The close association between the TTS topography and the hydrogen embrittlement phenomenon in pearlitic steels has recently been investigated with notched and precracked specimens, and is supported by the following experimental facts [9]. The microscopic features of the TTS mode resemble microdamage or microcracking due to the hydrogen. The TTS mode appears only at cathodic potentials that correspond to hydrogen embrittlement environmental conditions. The size of the TTS region is directly influenced by the compressive residual stresses generated in the vicinity of the crack tip during the fatigue precracking procedure, because these residual stresses delay the hydrogen entry into the sample. The size of the TTS region is an increasing function of the test duration (directly related to the time for hydrogen diffusion). Finally, the asymptotic depth of the TTS region for quasi-static tests reaches

the point of maximum hydrostatic stress in the sample, which confirms that hydrogen diffuses towards the points of maximum hydrostatic stress.

The correlation between the TTS and hydrogen effects gives an approach to clarifying which is the main mechanism of hydrogen transport in pearlitic steels. The TTS size has to be compared with the distribution of hydrostatic stress in the sample or with the extension of the plastic zone, depending on the mechanism of hydrogen transport under consideration. If lattice diffusion were the predominant mechanism, then the hydrostatic stress would be an outstanding variable. On the other hand, if hydrogen were mainly transported by dislocation sweeping, then the evolution and size of the plastic zone would be relevant, since outside that zone there is no movement of dislocations.

In this research a commercial hot-rolled pearlitic steel supplied in bar form of 12 mm diameter was used. This steel presents a coarse pearlitic microstructure (austenite grain size 75 μm and pearlite interlamellar spacing 0.3 μm). The 0.2% offset yield strength, $\sigma_{0.2}$, is 600 MPa and the ultimate tensile strength (UTS) 1200 MPa. The stress-strain curve can be modelled according to the Ramberg-Osgood expression $\epsilon = \sigma/199\,000 + (\sigma/2100)^{4.9}$, where σ is in MPa.

Axisymmetric notched samples were machined from the 12 mm diameter bars after producing cylinders of diameter 11.25 mm. A broad range of geometries was covered in the general programme [9, 10], but this study focused on a specific geometry in which it is easy to distinguish the effects of the hydrostatic stress distribution and the spreading of the plastic zone. The elastic-plastic analysis [10] demonstrated that the geometry of minimum notch radius and maximum notch depth was adequate for this purpose. This notched geometry is depicted in Fig. 1.

The hydrostatic stress distribution for the chosen geometry is shown in Fig. 2 for a loading step after elastic regime. The hydrostatic stress levels change with the loading process, but the point of maximum hydrostatic stress always remains at depth x_S (characteristic of the geometry) from the notch tip, as demonstrated in [10]. For the geometry considered here this point is placed at the centre of the net section (the bar axis).

The spreading of the plastic zone is shown in Fig. 3 for different values of the external displacement applied to the sample ends. It develops narrowly in

*Present address: Department of Engineering, University of La Coruña, E.T.S.I. Caminos, Pol Sabón, P. 12-14, 15141 Arteixo, La Coruña, Spain.

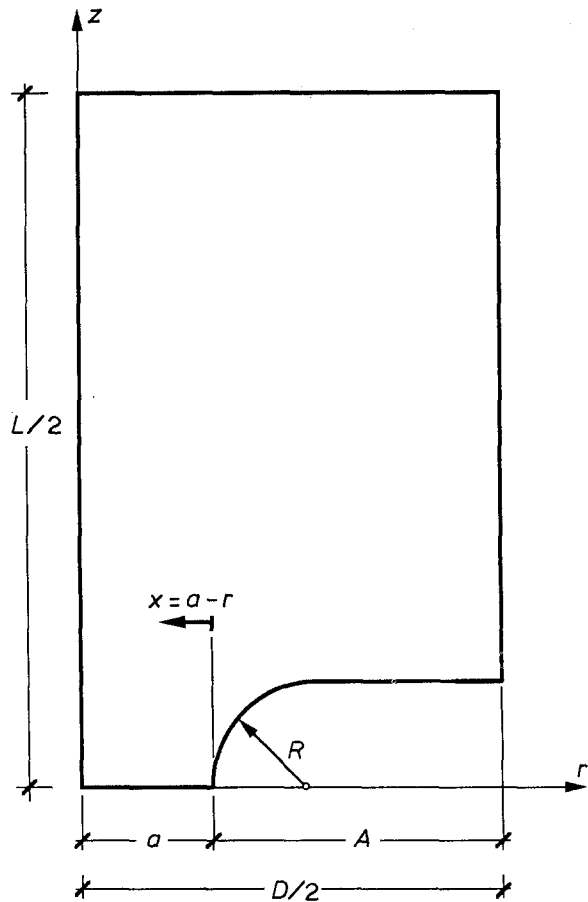


Figure 1 Notched geometry ($R/D = 0.05$, $A/D = 0.39$; $L/D = 4$ in the computations; and $D = 11.25$ mm in the tests).

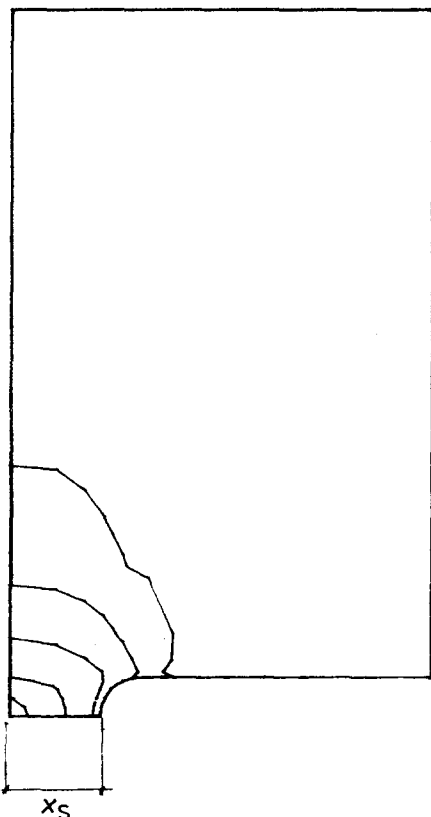


Figure 2 Hydrostatic stress distribution in the sample (after elastic regime), where x_s is the depth of the maximum hydrostatic stress point.

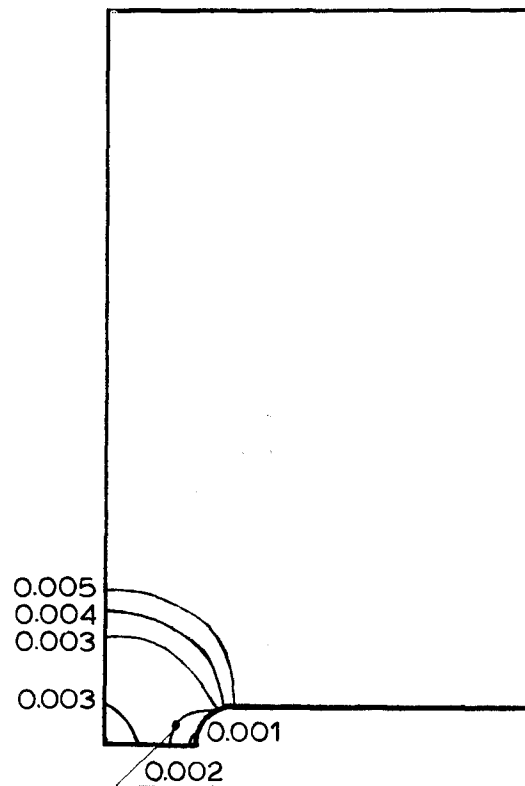


Figure 3 Spreading of the plastic zone, for different values of u/D , where u is the displacement applied to the sample ends ($L = 4D$) and D is the sample diameter.

comparison with the other geometries analysed in [10] (results from the elastic-plastic computations), which allows a restriction of the hydrogen transport by dislocation movement in a certain area.

Therefore, for the purposes of the present analysis the main advantage of the chosen geometry is that hydrogen is attracted to the centre of the section, thus producing a broader affected region detectable by fractographic analysis, while providing a plastic zone sufficiently small to restrict the movement of dislocations to a reduced area. The probability of detecting hydrogen effects outside the plastic zone is high in this type of sample.

To obtain experimental data about the hydrogen-affected area in the samples, and compare them with the hydrostatic stress distribution and with the extension of the plastic zone, slow strain rate tests (SSRTs) were performed in an aqueous medium which promoted hydrogen embrittlement. The test environment was an aqueous solution of 1 g l^{-1} $\text{Ca}(\text{OH})_2$ plus 0.1 g l^{-1} NaCl , with a pH of 12.5. All tests were performed at room temperature with potentiostatic control at a constant potential of -1200 mV versus saturated calomel electrode (SCE) by means of a potentiostat and a classical three-electrode assembly, as described elsewhere [9]. A broad range of displacement rates (between 10^{-9} and 10^{-6} m s^{-1}) was covered in the SSRTs to evaluate different degrees of hydrogen damage on the samples.

As reported previously [9], there is a specific microscopic mode of fracture, the TTS, associated with the hydrogen embrittlement process. This is not only a fracture mode, but also a propagation mode

in hydrogen-assisted cracking processes. The extension of the TTS zone gives an estimate of the hydrogen-affected area, and it can be compared with the spreading of the plastic zone and with the hydrostatic stress distribution.

Table I gives the experimental results of the SSRTs the displacement rate (\dot{u}), time to failure or critical time (t_c), depth of the TTS region (x_{TTS}) and the extension of the plastic zone (x_{PZ}) at the end of each test. In the majority of cases the plastic zone (PZ) clearly exceeds the hydrogen-affected region (TTS) and does not have any relationship with it, which is consistent with previous results for very different notched geometries [10]. This experimental fact does not prove anything about the hydrogen transport by dislocation sweeping, since the TTS region is completely surrounded by the plastic zone in which dislocations move. It proves only that there is no net balance of hydrogen transport in the whole extension of the plastic zone. Nevertheless, for the geometry described in this letter ($R/D = 0.05$ and $A/D = 0.39$) and for the two slowest tests, the situation is the opposite; in this case the hydrogen-affected area (TTS) overpasses the only region in which there is dislocation movement, and the hydrogen transport cannot be attributed to dislocation dragging, but only to a random-walk diffusion. It is not, however, conventional diffusion according to the classical Fick's laws, but stress-assisted diffusion in which the hydrostatic stress field plays a very important role in accelerating the diffusion and enlarging the penetration distance. It is significant that the depth of the TTS region in the slowest test

(quasi-static) almost reaches the point of maximum hydrostatic stress, a general result for all geometries [10]. For the particular geometry described here, this point is exactly at the centre of the sample.

The above considerations do not attempt to refute hydrogen transport by dislocation sweeping. No conclusion can be drawn about this topic (if any, only the difficulty of demonstrating that there is a net transport towards a specific site where fracture initiates). This letter provides only experimental evidence of hydrogen transport by diffusion in pearlitic steel, in which hydrogen diffuses towards the points of maximum hydrostatic stress, its effect being clearly detectable by fractographic analysis after failure.

Acknowledgements

The author thanks Dr A. M. Lancha (Polytechnical University of Madrid) for the scanning electron microscopy and Mr J. Monar (Nueva Montaña Quijano Company, Santander, Spain) for providing the steel used in the experimental programme. Support for this work was provided by the Polytechnical University of Madrid under grant A9000200161.

References

1. R. N. PARKINS, M. ELICES, V. SANCHEZ-GALVEZ and L. CABALLERO, *Corros. Sci.* **22** (1982) 379.
2. H. H. JOHNSON, J. G. MORLET and A. R. TROIANO, *Trans. Met. Soc. AIME* **212** (1958) 528.
3. A. R. TROIANO, *Trans. ASM* **52** (1960) 54.
4. J. K. TIEN, A. W. THOMPSON, I. M. BERNSTEIN and R. J. RICHARDS, *Met. Trans.* **7A** (1976) 821.
5. H. H. JOHNSON and J. P. HIRTH, *ibid.* **7A** (1976) 1543.
6. A. J. WEST and M. R. LOUTHAN, JR, *ibid.* **13A** (1982) 2049.
7. T. ZAKROCZYMSKI, *Corrosion* **41** (1985) 485.
8. A. W. THOMPSON and J. C. CHESNUTT, *Met. Trans.* **10A** (1979) 1193.
9. J. TORIBIO, A. M. LANCHA and M. ELICES, *Corrosion* **47** (1991) 781.
10. *Idem, Mater. Sci. Engng A145* (1991) 167.

Received 1 October 1991
and accepted 6 February 1992

TABLE I

\dot{u} (m s^{-1})	t_c (s)	x_{TTS} (mm)	x_{PZ} (mm)
1.00×10^{-7}	720	0.10	Net section
1.03×10^{-7}	780	0.15	Net section
1.02×10^{-8}	5760	0.25	Net section
8.70×10^{-9}	7380	0.21	Net section
6.90×10^{-9}	8520	0.27	Net section
6.23×10^{-9}	11 160	0.30	Net section
6.02×10^{-10}	75 600	0.60	Net section
1.87×10^{-10}	143 040	0.93	0.33
1.12×10^{-10}	262 800	1.00	0.41